# Errors in light sheet images of polydisperse sprays: Monte Carlo simulation of photon propagation

by

M.C. Jermy, E. Berrocal and F. Moukaideche

DAMSE

School of Engineering

Cranfield University

Cranfield

Beds MK43 0AL

United Kingdom

[(1)]E-Mail: m.jermy@cranfield.ac.uk

**ABSTRACT**

In light sheet imaging of sprays, single scattering is usually assumed. However in dense sprays significant multiple scattering can occur. This gives rise to errors in the data extracted from the image. To quantify these errors we have written a Monte Carlo photon transport code capable of simulating the propagation of light and the resultant image in three-dimensional, polydisperse sprays. The code has been used to establish the amount of multiple scattering in a typical gas turbine airblast fuel injector spray and the effects on the photons reaching the camera. These effects include broadening of the light sheet, and a position dependent attenuation of the scattered signal by the spray lying between the light sheet and the camera.

The code has been used to calculate the amount of multiple scattering affecting a light sheet imaging experiment of a dense spray from a gas turbine fuel injector. Experimental data on the droplet size and concentration has been used to ensure the simulation is realistic. Only 3% of the photons reaching the camera are singly scattered. Photons that reach the camera have been scattered, on average, seven times. This will cause significant errors in the liquid volume fraction measured from the image, if single scattering is assumed. The detector acceptance angle can be used to reduce the multiple scattering contribution by around one fifth.

The attenuation of the signal light by the spray lying between the light sheet and the camera has been measured experimentally in a hollow cone spray by a backlighting method. This attenuation is position dependent and of order tens of percent, even at low spray density. However this attenuation can be corrected in light sheet images with the attenuation map generated by the backlighting method.

## 1. INTRODUCTION

In light sheet imaging of sprays it is usual to assume single scattering i.e. each photon that reaches the camera has scattered from only one droplet. However the denser the spray the greater the fraction of photons which have scattered from more than one droplet, some of which droplets may lie outside the light sheet. The information these photons carry on the structure and droplet size of the spray is ambiguous. This multiple scattering causes blur, loss of contrast and attenuation (photons not reaching the camera, which would have reached it if they had scattered from only one droplet) as well as effectively broadening the light sheet.

Multiple scattering is difficult to investigate experimentally as it is difficult to determine how many times a detected photon has scattered. However if photon propagation is simulated, the history of each photon is known. Simulations can be deterministic (e.g. Rozé et al. 2001) or stochastic. In stochastic (i.e. Monte Carlo) simulations the position and angle of each scattering event are determined by generating random numbers and comparing these to the known probabilities of scatter and of angle of deflection from the appropriate single particle scattering theory (e.g. Mie theory or Rayleigh approximation).

The technique has been applied successfully to biological media (e.g. Wang et al. (1995) Kandidov (1996) and Meglinsky and Matcher (2001), clouds (e.g. Marchuk et al. (1980), Lavigne et al. (1999) and ground level fogs (Girasole et al. 1998).

In this paper we report a Monte Carlo code capable of simulating the propagation of photons in three-dimensional polydisperse particle fields, in which the particle size distribution may vary with position in the spray. The code is used to determine the effect of multiple scattering on the image of a typical gas turbine airblast atomizer fuel spray. Experimental results of the attenuation of the scattered signal light by spray lying between the light sheet and the camera are also presented.

## 2. SIMULATIONS

### 2.1 Light sheet imaging geometry and terminology

The geometry of a typical light sheet imaging experiment is shown in Fig. 1. The light sheet illuminates a plane of the spray. In practice multiple scattering will cause the light sheet to broaden as it propagates through the spray. This means droplets may be scattered more than once in the light, and may subsequently scatter from droplets outside the light sheet or may leave the spray without further scattering. The sheet is attenuated as it passes through the spray. This in-plane attenuation can be corrected by one of two types of techniques (Talley et al. (1996), Abu-Gharbieh et al. (2000)). Light scattered from the light sheet towards the camera may be scattered again by droplets outside the light sheet. This effect is related to the effect termed ‘radiation trapping’ in flames in which thermal radiation is scattered back into the flame by soot or fuel particles. In this paper this effect is termed ‘out of plane scattering’ (OOPS). OOPS is responsible for an attenuation of the light reaching the camera. The degree of attenuation depends on the structure of the spray along the path of the photon and so is not uniform across the image. Lastly, light scattered out of the light sheet, which would not reach the camera if it were not subsequently scattered, may be scattered into the camera by droplets anywhere in the spray. This effect causes a fairly uniform background intensity and a loss of contrast. This effect is similar to that responsible for the loss of contrast encountered when driving through fog.

The severity of the different types of errors depends on the structure of the spray, the droplet concentration, the droplet size and on the wavelength of light.

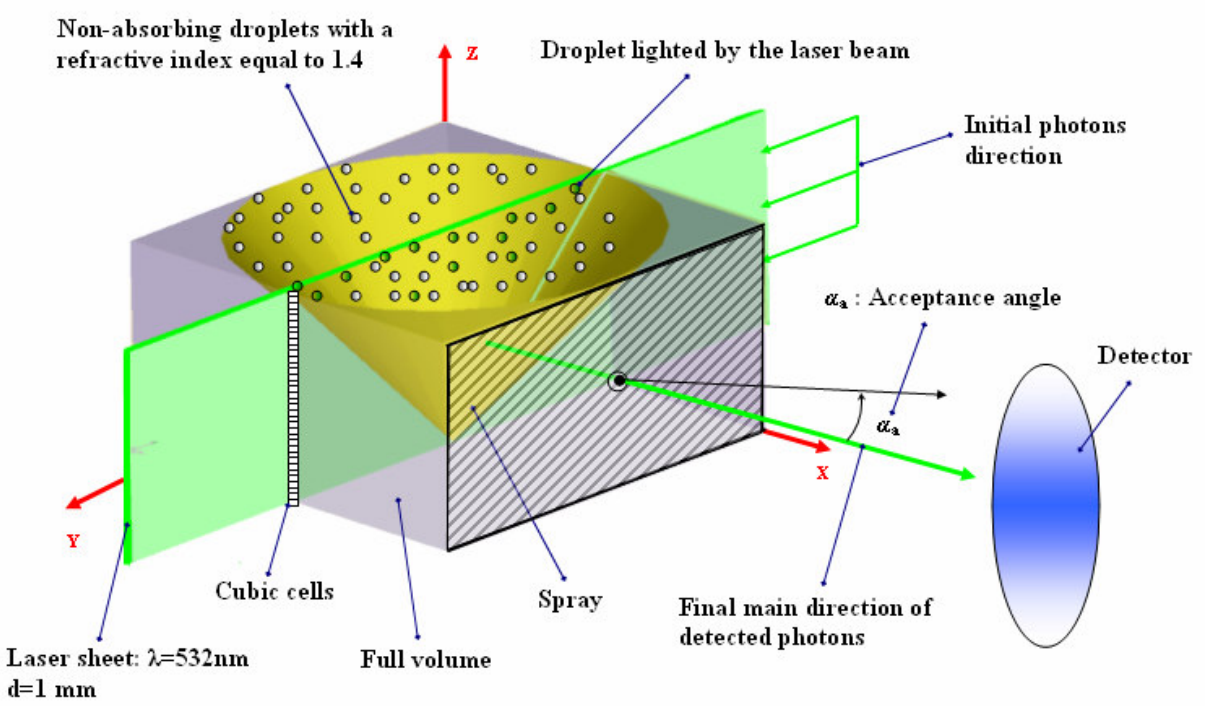


*Fig. 1: Typical light sheet experiment showing as an example a hollow cone spray, the light sheet and the camera lens*

## 2.2 Monte Carlo method

The Monte Carlo code used here, SATURN, was first described by Jermy and Allen (2002) since when it has been considerably improved. It is ideally suited to sprays problems as it can handle arbitrary geometries (does not require any symmetry in the droplet field). Speed and accuracy have been increased and the code can now simulate more than one scattering event in one cell. The code is unique in that it can now handle polydisperse sprays in which the droplet size distribution varies from place to place in the particle field.

The volume considered in the calculation is divided into cubic cells. Some of the cells are defined as sources and assigned a strength and direction of emission. Photons leaving the source cells are tracked through the calculated volume. The distance $l$ the photon travels between scattering events is determined with Eq. 1

$$l = \frac{-\ln \xi_1}{\mu_s} \qquad \text{Eq. 1}$$

where $\xi_1$ is a random number uniformly distributed between 0 and 1 and $\mu_s$ is the scattering coefficient of the medium. $l$ is modulated according to the changes of $\mu_s$ from cell to cell.

Since the particle field is polydisperse, the scattering coefficient in each cell $\mu_s$ depends on the number density and scattering cross section of the particles in that cell, according to Eq. 2

$$\mu_s = \sum_i n_i \sigma_i \qquad \text{Eq. 2}$$

where $n_i$ is the number density and $\sigma$ the scattering cross section of particles of size i.

When the photon is scattered the direction of scatter is determined from the cumulative probability distribution function CPDF(x) where x is $\theta$ the scattering angle or $\phi$ the azimuthal angle according to Eq. 3.

$$\xi_2 = CPDF(\theta)$$
$$\xi_3 = CPDF(\phi) \qquad \text{Eq. 3}$$

where $\xi_2$ and $\xi_3$ are random numbers distributed uniformly between 0 and 1 and independent of $\xi_1$ and of each other. In this paper the scattering is in the Mie regime, so CPDF(θ) is derived from the phase function p(θ,a) calculated from Mie theory with the far field Mie scattering package LightLab 1.0 (Valley Scientific) and normalized according to Eq. 4.

$$CPDF(\theta) = \frac{\int_0^{\theta} p(\theta', a)d\theta'}{\int_0^{\pi} p(\theta', a)d\theta'} \qquad \text{Eq. 4}$$

where the phase function for a single particle size is p(θ,a) where a is the size parameter of the particle $a=\pi d/\lambda$, d the diameter of the particle and λ the wavelength of the source. When a scattering event occurs, for a truly polydisperse calculation the particle size is selected using the local size distribution PDF and a random number, and the appropriate phase function selected. However to reduce calculational time, in the calculations presented here the size of each scattering particle is always set equal to the SMD of the cell and the phase function from the appropriate size class used. This neglects the effect of the different phase functions of the smaller and larger particles.

The size is selected from 24 size classes. The size classes are chosen so that the phase function at the extreme sizes of each class are not dissimilar. For each class the corresponding CPDF has been calculated with LightLab 1.0. CPDF(θ) for each size class are shown in Fig. 2.

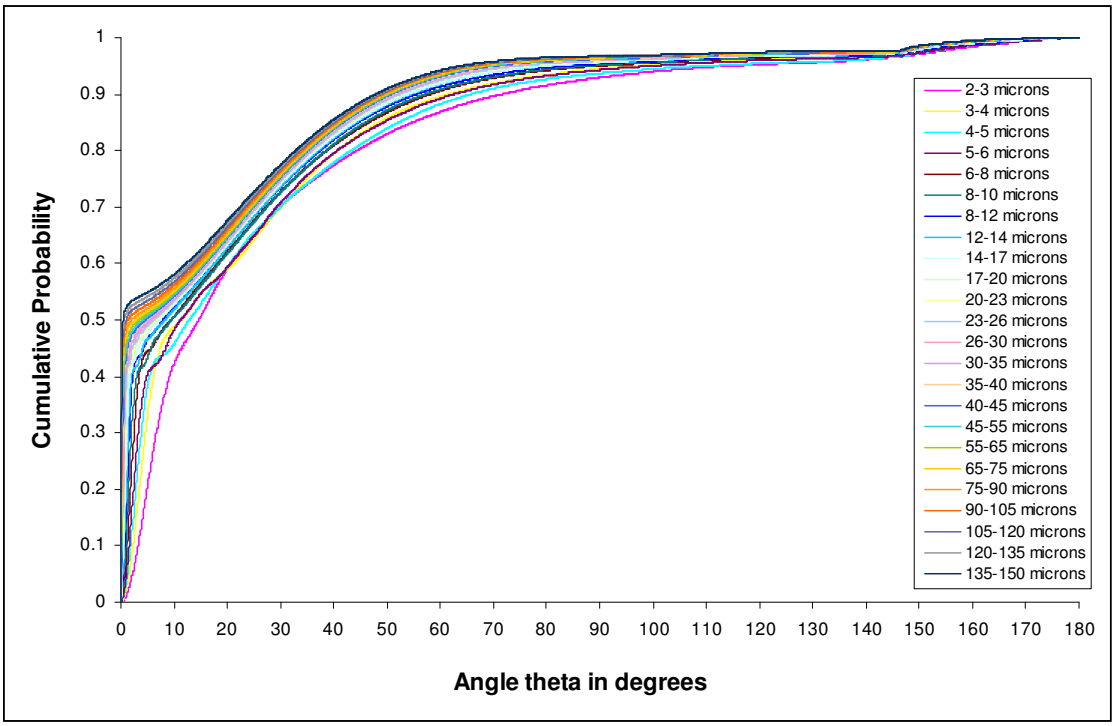


*Fig. 2: CPDF(θ) for the 24 size classes*

In this paper the source is unpolarised so CPDF(ϕ) is linear between 0 at 0 radians and 1 at 2π radians.

Once the photon's new direction is determined, it's path length to the next scattering event is determined with Eq. 1 and the process repeats until the photon leaves the simulated volume. On exit, the properties of the photon are recorded. These include the final position, the final direction, the total path length and the number of times scattered. These properties are compared to the properties of the detector. Any detector may be simulated from a simple areal photon counter to a true camera with defined f/# and acceptance angle. Detectors may include filters for the number of times scattered so that the calculated signal contains only single scattered photons, only doubly scattered photons, and so on.

## 2.2 Validation

The code has been validated by comparing SATURN calculations with a code developed by T. Girasole and C. Rozé and co workers of CORIA, Rouen. This code handles polydisperse media by means of a phase function averaged over the particle size distribution (Girasole et al. 1998). SATURN differs in that it can handle size distributions which vary with position in the spray.

The validation calculations featured a square beam of light passing through a cubic volume containing a homogenous distribution of droplets. The statistics of the photons emerging through the faces of the cube were calculated. The difference between the codes was within the random error expected from the number of photons sent.

SATURN results have also been compared with theory for a crossed source-detector geometry and isotropic scattering. The two agree well (Meglinski et al. 2004).

## 2.3 Monte Carlo simulations

SATURN has been used to simulate the scattering of the laser light in a light sheet imaging experiment on a gas turbine airblast atomiser spray. The number concentration and droplet size information was derived from experiment, from calibrated light sheet image data from a gas turbine airblast atomizer fuel injector. The atomizer was run in the Cranfield 7 bar sprays rig. This rig can reach a maximum pressure and temperature of 7 bar, 200$^{o}$C and the compressors can provide an air flow up to 2 kgs$^{-1}$. The rig has a siren to impose an acoustic perturbation on the spray if required. For this data an air pressure of 3 bar was used in the main chamber, with a pressure drop across the atomizer of 5% of the chamber pressure, and a fuel flow rate of 6gs$^{-1}$. The fuel was Exxsol D-80, a kerosene substitute with low UV absorbance, doped with 0.012gl$^{-1}$ m-terphenyl. The measurements are described in detail in Greenhalgh et al (2004). This concentration is chosen according to the principles laid out in Jermy and Greenhalgh (2000). The number concentration and droplet size (actually Sauter Mean Diameter) are measured with Laser Induced Fluorescence (LIF) and LIF/Mie image ratioing (Jermy and Greenhalgh 2000).

The beam from a 248nm KrF Lambda Physik CompEx 110 excimer laser was formed into a sheet ≈50mm high and 1mm thick which passed through the centreline of the spray. Each pulse was 100mJ. The light scattered by the droplets was collected by a Princeton Instruments 'ICCD' intensified CCD camera. The intensifier gate width was 200ns. The camera had a Nikon 105mm UV lens at f/4.5. A four-mirror system projected both a LIF and a Mie image on to the camera chip, side by side and simultaneously. The Mie image was filtered with a 248nm band pass filter and the LIF with a Schott BG filter.

The LIF and LSD images can be calibrated to yield fully quantitative values of AFR and SMD in each pixel. The calibration is done by taking images of a droplet field with known SMD and AFR. The known droplet field is the stream of droplets from a Berglund-Liu type vibrating orifice monodisperse droplet generator. This generates a stream of droplets all of the same size and spacing. The size and spacing are measured with a travelling microscope and with a Phase Doppler Anemometer (PDA).

100 single shot images are collected with laser passing one way through the spray. Then the injector is rotated and 100 images taken with the laser passing the opposite direction. Each set of 100 images is averaged. The two averaged images are combined according to the method of Talley et al. (1996). This corrects for the in-plane attenuation of the light sheet as it passes through the spray.

Fig. 3 shows the corrected images of liquid volume fraction and Sauter Mean Diameter. Typical SMDs are ≈20μm in the centre of the recirculation zone, and 35-40μm near the nozzle exit. Typical liquid volume fractions are 0.15% in the centre of the recirculation zone.

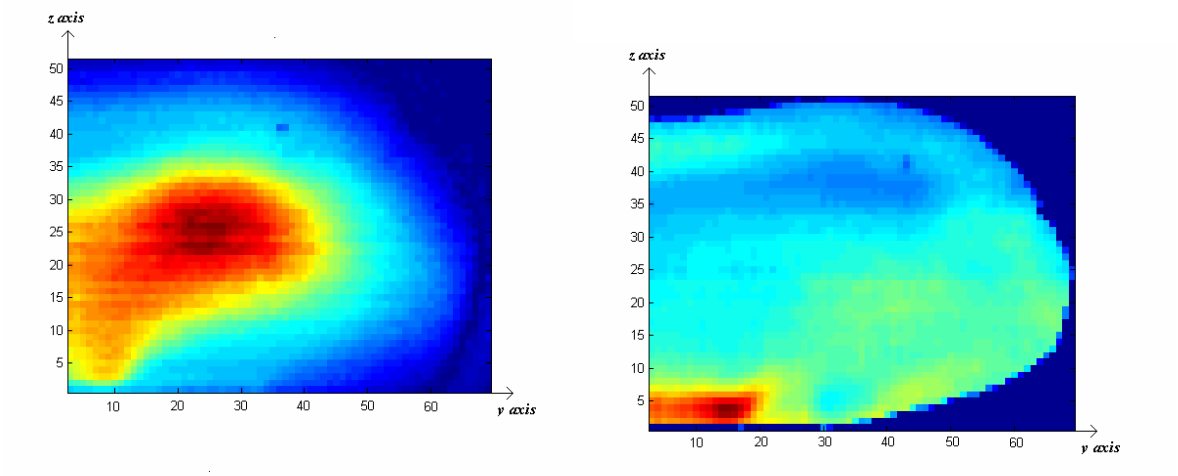


*Fig. 3: False colour images of (a) liquid volume fraction and (b) Sauter Mean Diameter of the spray used in the simulations. Scale is number of cells.*

The number concentration and droplet size obtained from this method suffer from all the systematic errors related to multiple scattering described above. The effect expected to be most significant is OOPS affecting the structure of the image and hence the inferred structure of the spray. Two effects are expected. Rescattering of photons will affect the structure of the image. OOPS will also attenuate the light levels reaching the camera, introducing errors in the liquid volume fraction calibration constant and hence the inferred number concentration. However since the AFR values given by the data are plausible the errors must be of sufficiently low magnitude that the data yields a useful estimate of the spray droplet size and concentration as a starting point for investigation. The OOPS attenuation can be corrected in future by using the method described in section 3 below to measure the OOPS and correct it during image processing.

In any one cell, it is assumed that all droplets have diameter equal to the SMD and scatter with the phase function of the size class containing the SMD.

The data shown in Fig. 3 is rotated about the z axis to generate the full volume of the spray.

Two simulations are performed. One includes the full volume of the spray. The other includes only a slice 1 cell (558μm) thick in the illuminated plane. Since in this simulation there is no spray lying between the illuminated plane and the camera, there is no OOPS. Comparing the results of the two simulations shows the effects of OOPS on the scattered photons.

The full volume simulation has a matrix of 131x131x50 cubic cells of side 558μm.

For both calculations, 10 million photons were simulated.

## 2.4 Monte Carlo results

Fig. 4 shows the percentage (of the total number of photons detected on the X max face) in each scattering order. Scattering order zero contains unscattered photons, order 1 those photos which have been singly scattered, and so on. The X max face is parallel to the plane illuminated by the laser sheet (Fig. 1). In a light sheet imaging experiment with $90^{o}$ viewing angle the camera would be looking through this face.

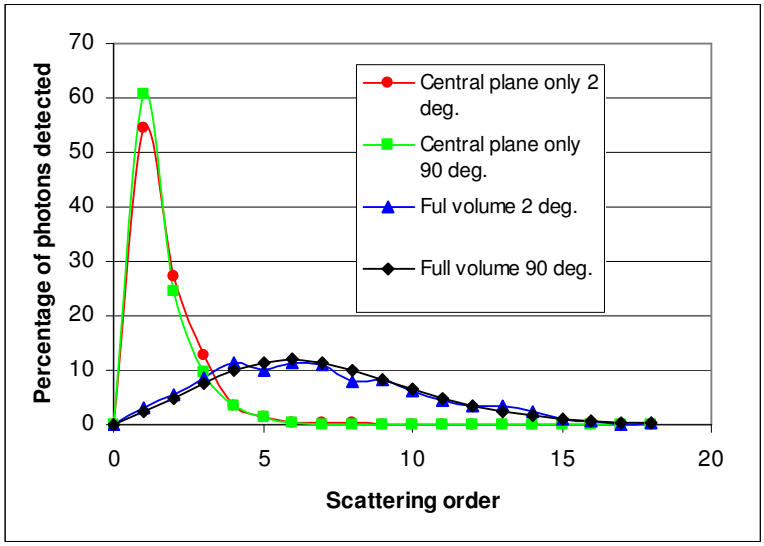


*Fig. 4: Percentage (of photons detected) in each scattering order for scattering orders 0-18*

Both the central plane only and the full volume simulations show a skewed Gaussian form to this plot but as expected the full volume plot has its peak at a much higher scattering order. In the full volume case the average photon has been scattered seven times before reaching the camera, so multiple scattering is a significant effect. In the case of the central plane only, the majority of photons have been scattered only once, as desired, though a significant number have been scattered twice. The majority of these will have been scattered in the forward direction once in the illuminated plane, and only on the second scatter have they left the illuminated plane in the direction of the camera.

The curves in Fig. 4 are plotted for acceptance angles of $2^o$ and $90^o$. A photon is included in the results only if (1) it exits through the X max face and (2) its trajectory makes an angle to the X axis less than the acceptance angle. Acceptance angle of a camera system is determined by the lens (principally by the aperture). The acceptance angle makes little difference to the scattering order curve for these simulations. For the full volume case, the $2^o$ acceptance angle curve is less smooth than the $90^o$, simply because less photons are accepted and the statistical fluctuations are greater.

Fig. 5 (a) plots I(1)/I(tot) vs. acceptance angle. I(1) is the intensity of the 1st order scattering and I(tot) the intensity of all orders. Detection is through the X max face.

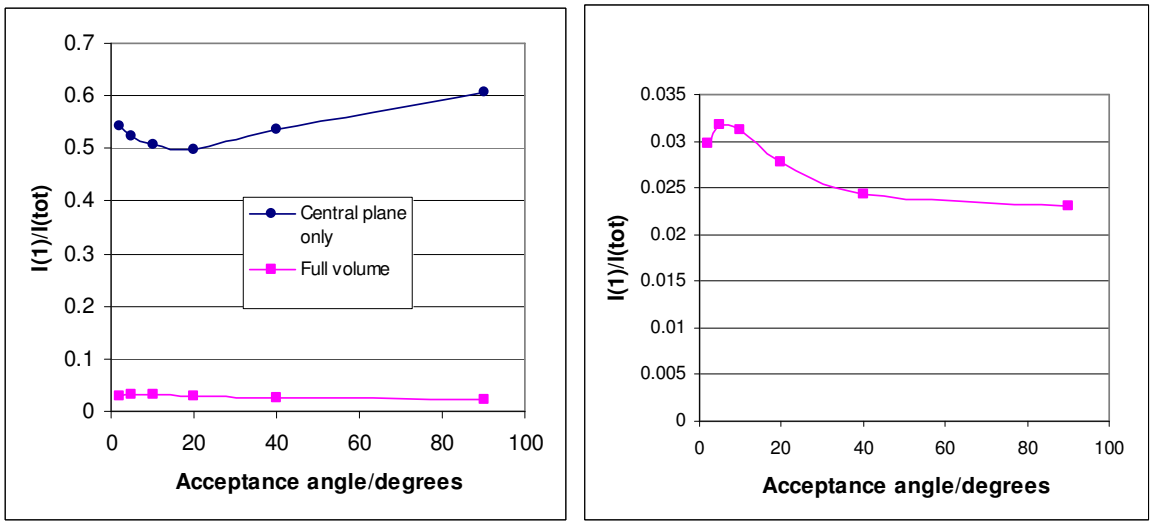

*Fig. 5: I(1)/I(tot) vs. acceptance angle for (a) both simulations and (b) the full volume simulation on an expanded Y axis*

I(1)/I(tot) is a measure of how much single scattering dominates. To minimise the errors described in section 2.1 errors in light sheet imaging results I(1)/I(tot) should be as high as possible. For the image to contain effectively single scattering only, I(1)/I(tot) must be greater than 0.5.

The values of I(1)/I(tot) are naturally lower at ≈0.03 for the full plane calculations with the greater degree of multiple scattering, so it is plotted on Fig. 5(b) on an expanded Y axis.

The values are much higher for the central plane only simulation, at ≈0.5 indicating that about 50% of the photons reaching the camera have been scattered only once.

In both cases I(1)/I(tot) is sensitive to acceptance angle. The central plane only calculation shows a minimum at around $20^o$ with a variation of about one fifth of the typical value over the 0-$90^o$ range of acceptance angles. The full volume calculation in contrast shows a maximum, at ≈$5^o$, again with a variation of about one fifth of the typical value. The presence of a maximum and the degree of variation are similar to those found in an earlier Monte Carlo investigation of the effect of camera aperture on I(1)/I(tot) in a monodisperse spray of similar geometry (Jermy et al. 2002b).

With isotropic scattering, it is possible to get higher values of I(1)/I(tot) by judicious choice of the detector viewing and acceptance angles (Meglinski et al. 2004) as subsequent scatters tend to scatter the photon out of the detector line of sight.

The degree of multiple scattering is extremely high in the full volume simulation. The degree of multiple scattering is affected by the choice of acceptance angle, but not sufficiently to restore virtual single scattering in a light sheet experiment on a spray of this density. The difference between the full volume and central plane only simulations shows that the bulk of the multiple scattering occurs outside the illuminated plane (OOPS). This may cause significant errors in interpretation of light sheet images of such sprays. However if the second and subsequent scatters are forward dominated, the image may be little affected as the multiple scattering will not deviate the photon far from the trajectory it would follow if it remained singly scattered as was found in Jermy et al. (2002b). However in this work the spray was less dense and the average number of scatters was small, ≈2. The greater the average number of scatters (≈7 in this case) the greater the deviation of the photons and the greater the errors in interpretation of the image. Future work will use the Monte Carlo results to simulate images of the spray and investigate the errors generated by interpreting the images with the assumption of single scattering.

## 3. MEASUREMENT OF OUT-OF-PLANE SCATTERING

The attenuation due to out-of-plane scattering is measured in the spray generated by a pressure swirl nozzle of the type used in oil fired boilers. The spray is lit from behind with a 500W halogen floodlamp behind a ground Perspex diffuser (Fig. 6). An image of the diffuser is taken with the camera focussed on the spray. The camera is a LaVision SprayMaster 3. Images are taken with the spray turned on and turned off. The fractional attenuation through the spray in any one pixel of the image is given by Eq. 5

$$\text{Fractional attenuation} = \frac{I_{off} - I_{on}}{2I_{off}} \qquad \text{Eq. 5}$$

where $I_{off}$ is the pixel intensity with the spray off, $I_{on}$ is the pixel intensity with the spray on.

The nozzle is fed with deionised water at 20 bar and sprays into a chamber at atmospheric pressure. The spray off images is shown in Fig. 6a, spray on in Fig. 6b. The image of fractional attenuation is shown in Fig. 7 along with the colour scale. White (maximum intensity) is at 32% attenuation and black at 0% attenuation.

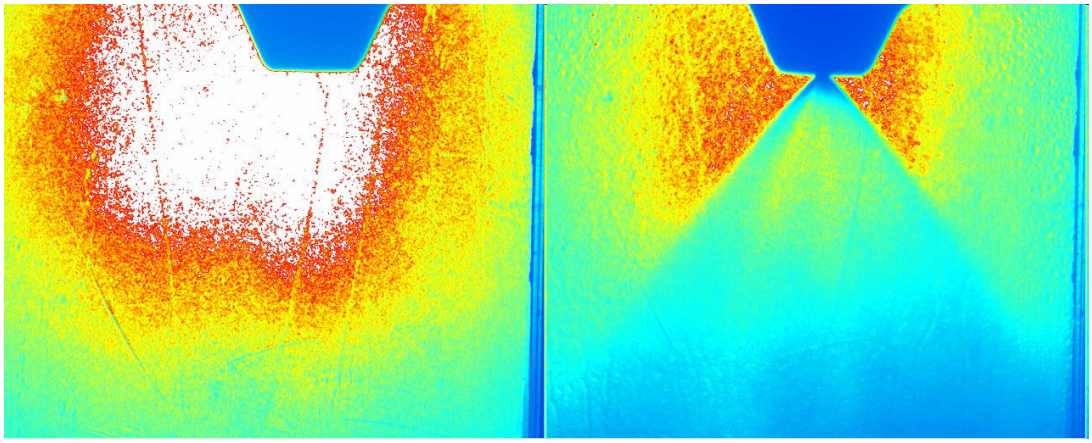

*Fig. 6: backlit images with (a) spray off and (b) spray on, fuel pressure 20 bar*

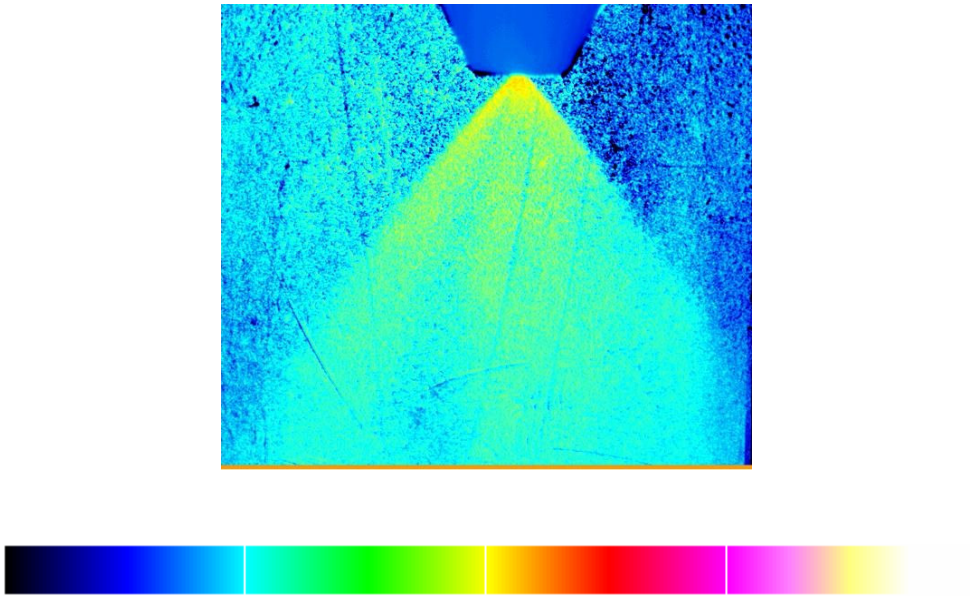

*Fig. 7: Map of out of plane attenuation generated by applying Eq. 5 to Figs. 6 (a) and (b). Colour scale is shown with maximum (white) at 32% and minimum (black) at 0%.*

The attenuation of the light by the spray between the illuminate plane and the camera is of order tens of percent. The attenuation is clearly position dependent, most severe in the densest parts of the spray (near the nozzle and at the edge of the spray).

The attenuation was measured at several water pressures. The maximum attenuation at each pressure is given in Table 1.

| **Pressure (bar)** | **4** | **5** | **6** | **7** | **8** | **20** |
|---|---|---|---|---|---|---|
| **Attenuation (%)** | **14** | **15.6** | **16** | **18.5** | **17** | **22** |

*Table 1: Maximum attenuation due to out of plane scattering, versus fuel pressure*

The attenuation increases with water pressure, naturally, but even at low pressures the maximum attenuation is 16%.

This level of attenuation will lead to significant errors in the droplet of liquid volume fraction measurements based on calibrated light sheet imaging. The errors will be of order tens of percent in sprays of similar scattering power to that measured here. However this backlit attenuation measurement used here can be used to determine the attenuation for any spray, and to correct the error due to out of plane attenuation.

## 4. SUMMARY

In light sheet imaging of sprays, single scattering is usually assumed. However in dense sprays significant multiple scattering can occur. This gives rise to errors in the data extracted from the image. To quantify these errors we have written a Monte Carlo photon transport code capable of simulating the propagation of light and the resultant image in three-dimensional, polydisperse sprays.

The code has been used to calculate the amount of multiple scattering affecting a light sheet imaging experiment of a dense spray from a gas turbine fuel injector. Experimental spray data has been used to ensure the simulation is realistic. The droplet phase function was assumed to be that of a droplet of diameter equal to the local SMD, although fully polydisperse calculations are possible and will be carried out in future. Only 3% of the photons reaching the camera are singly scattered. Photons that reach the camera have been scattered, on average, seven times. This will cause significant errors in the liquid volume fraction measured from the image, if single scattering is assumed. The detector acceptance angle can be used to reduce the multiple scattering contribution by around one fifth.

The attenuation of the signal light by the spray lying between the light sheet and the camera has been measured experimentally in a hollow cone spray by a backlighting method. This attenuation is position dependent and of order tens of percent, even at low spray density. However this attenuation can be corrected in light sheet images with the attenuation map generated by the backlighting method.

## ACKNOWLEDGEMENTS

We would like to thank Thierry Girasole and Claude Rozé of Complex de Recherche Interprofessionel en Aerothermie, CNRS UMR 6614 for useful discussions and for Monte Carlo calculations. We would like to thank the UK EPSRC for support under grant GR/R92653.

## REFERENCES

Abu-Gharbieh R., Persson J.L., Forsth M., Rosen A., Karlstrom A. and Gustavsson T. (2000), "Compensation method for attenuated planar laser images of optically dense sprays", Appl. Opt. **39**, 1260-1267

Girasole T., Roze, C., Maheu, B., Grehan, G. and Menard, J. (1998), "Visibility distances in a foggy atmosphere: comparisons between lighting installations by Monte Carlo simulation" Int. J. Lighting Research and Technology, 30, 29-36

Greenhalgh D.A., Jermy M.C. (2000), "Planar dropsizing by elastic and fluorescence scattering in sprays too dense for phase Doppler measurement", Appl. Phys. B **71** 703-710

Greenhalgh D.A., Jermy M.C., Doherty W.G. and Hussain M. (2004) "The response of fuel injector sprays to acoustic forcing", ASME paper ESDA 2004-58617

Jermy M.C. and Allen A. (2002), "Simulating the effects of multiple scattering on images of dense sprays and particle fields", Appl. Opt. 41, 4188-4196

Jermy M.C., Allen A. and Vuorenkoski A.K., (2002b) "Simulating the effect of multiple scattering on images of dense sprays", in "Optical and laser diagnostics, Proc. 1st Int. Conf." pp 89-94, IOP Conference Series No. 177, eds. C Arcoumanis and KTV Grattan, ISBN 07503 0958X

Kandidov V.P. (1996), "Monte Carlo Method in nonlinear statistical optics", Physics-Uspekhi **39** 1243-1272

Lavigne C., Robin, A. Outters V., Langlois S., Girasole T. and Roze C. (1999), “Comparison of iterative and Monte Carlo methods for calculation of the aureole about a point source in the Earth's atmosphere” Appl. Opt. **38**, 6237-46

Marchuk G.I., Mikhailov G.A., Nazaraliev M.A., Darbinjan R.A., Kargin B.A. and Elepov B.S. (1980), "The Monte Carlo method in atmospheric optics" Springer, Berlin

Meglinsky I.V. and Matcher S.J., (2001), "Modelling the sampling volume for skin blood oxygenation measurements" Med. Biol. Eng. Comput. **39**, 44-50

Meglinski I. V., Romanov V. P., Churmakov D. Y., Berrocal E., Jermy M. C. and Greenhalgh D. A. (2004) “Low and high orders light scattering in particulate media” Laser Physics Letters 1(8): 387-390

Roze, C., Girasole, T. and Tafforin, A.-G. (2001), “Multilayer four-flux model of scattering, emitting and absorbing media” Atmospheric Environment, **35**, 5125-5130

Talley D.G., Verdieck J.F., Lee S.W., McDonell V.G. and Samuelsen G.S. (1996), “Accounting for Laser Sheet Extinction in Applying PLIF to Sprays”. AIAA 96-0469

Valley Scientific ‘LightLab 1.0’, www.Bright.Net/~vsi

Wang L., Jacques S.L. and Zheng L. (1995), "MCML- Monte Carlo Modeling of Light Transport in Multi- Layered Tissues" Comput. Methods Programs Biomed. **47**, 131-146